

Flow around Clark-Y airfoil: Summary of EFD benchmark data and comparison with IIHR EFD data and CFD solution

Nobuaki Sakamoto, Colin J. Johnson, Stuart Brezinski, Marian V. Muste and Frederick Stern
IIHR-Hydroscience&Engineering, The University of Iowa

1. EFD benchmark data

[1] JACOBS E.N., STACK J., AND PINKERTON R.M., 1930 Airfoil pressure distribution investigation in the variable density wind tunnel, Langley Memorial Aeronautical Laboratory Report No. 353

[2] MARCHMAN J.F. AND WERME T.D., 1984 Clark-Y airfoil performance at low Reynolds numbers, In: proc. AIAA 22nd Aerospace Science Meeting, Jan. 9-12, Reno, Nevada, U.S.A.

[3] SILVERSTEN A., 1934, Scale effect on Clark-Y airfoil characteristics from NACA full-scale wind-tunnel tests, Langley Memorial Aeronautical Laboratory Report No. 502

[4] ZIMMERMAN C.H., Characteristics of Clark-Y airfoils of small aspect ratios, 1932, Langley Memorial Aeronautical Laboratory Report No. 431

The summary of EFD benchmark data is given in Table 1.

Table 1 Summary of EFD benchmark data

Reference	[1]	[2]		[3]	[4]
Digitized data	C_p and C_L	C_p , C_L and C_D		C_L and C_D	C_L and C_D
AR*	7.2	5.75		6	0.5, 0.75, 1, 1.25, 1.5, 2, 3, 6
Re**	3.56e5	C_p	7.5e4	1.12e6, 1.55e6, 2.06e6, 2.81e6, 3.19e6, 3.59e6	8.6e5
		C_L , C_D	5e4, 7.5e4, 1e5, 2e5, 6.7e6		
α (deg)***	1, 4, 7, 10,13, 17, 20	C_p	0, 4, 6, 8, 12, 14	0, 1, 2, 3, 4, 5, 6, 7, 8, 9, 10, 11, 12, 13, 14, 15, 16, 17, 18, 19, 20, 21, 22, 23	0, 10, 15, 20, 25, 30, 35, 39, 40, 42, 50, 60
		C_L , C_D	0, 4, 6, 8, 12, 14		
Wingtip		End plates		Wing cross section	Rectangular

*: Aspect ratio, **: Reynolds number, ***: Angle of attack

2. Trend of each data set

2.1 Reference [1]

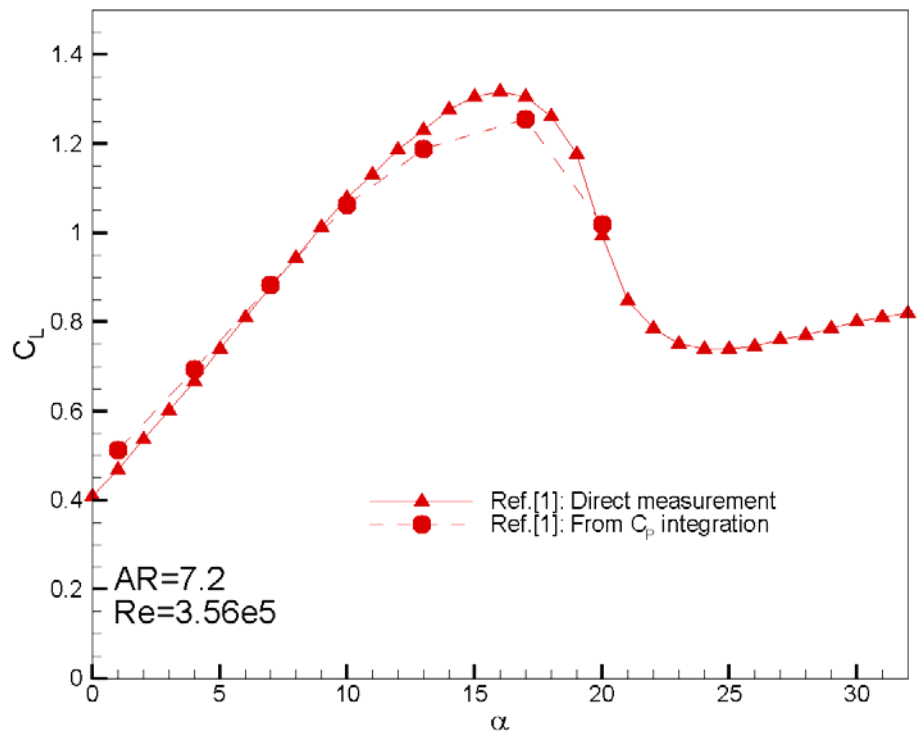


Fig. 1 Trend of C_L in Reference [1]

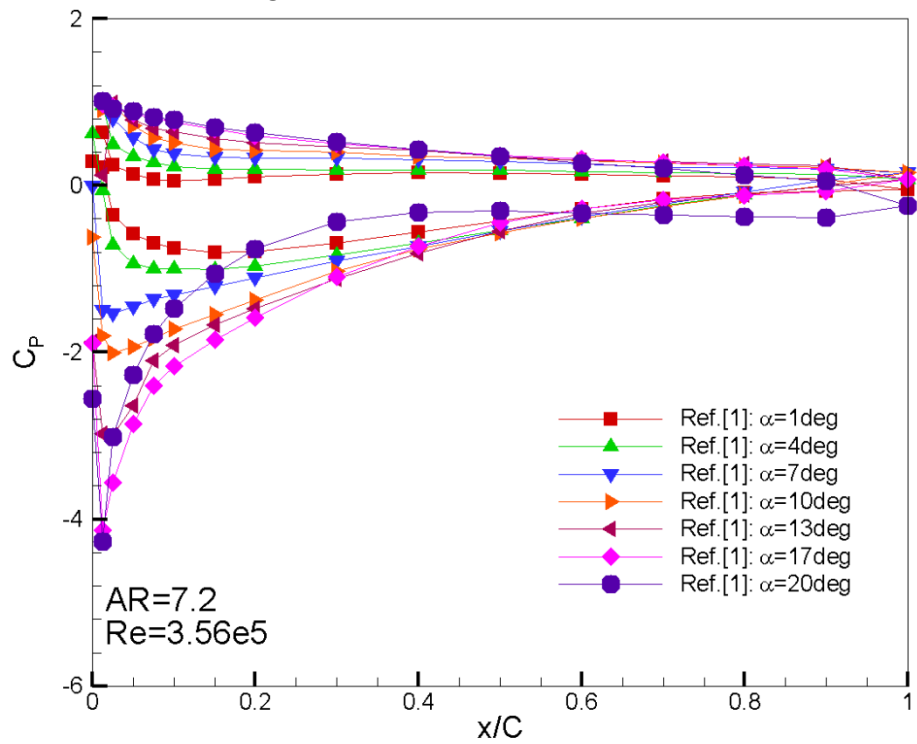


Fig. 2 Trend of C_p in Reference [1]

2.2 Reference [2]

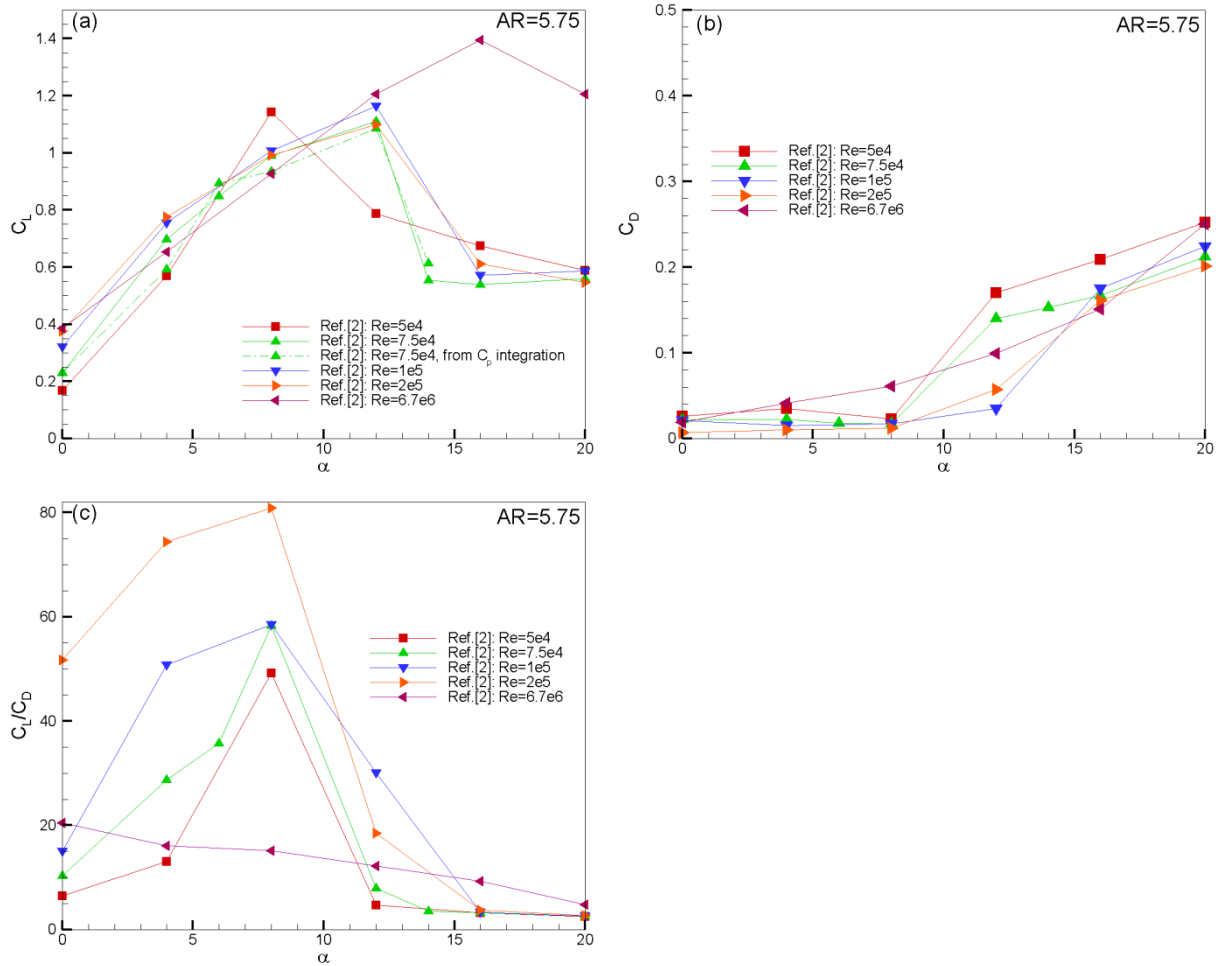


Fig. 3 Trend of C_L , C_D , and C_L/C_D with variations of Re in Reference [2]
 (a) C_L vs α , (b) C_D vs α , (c) C_L/C_D vs α

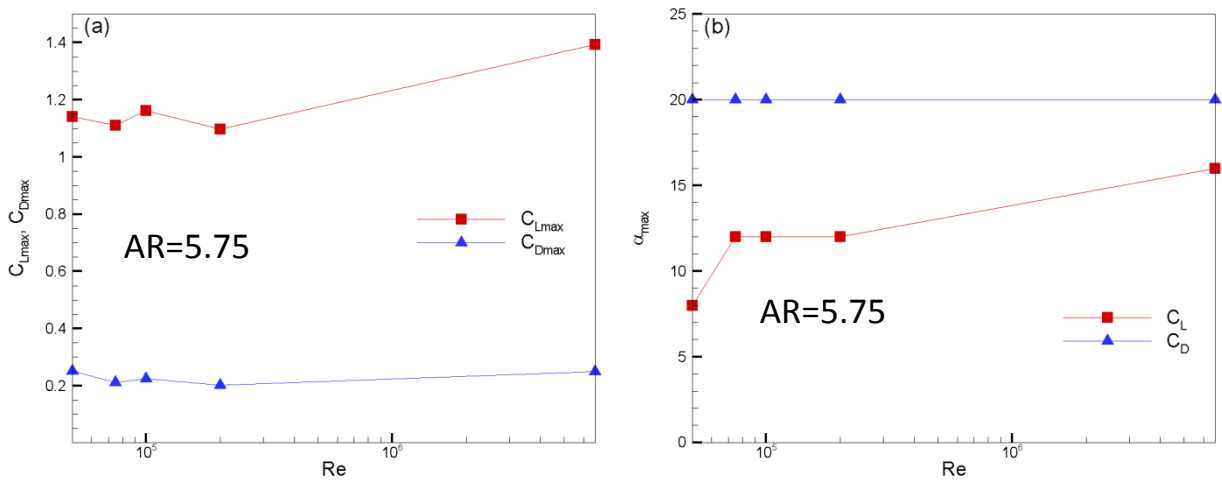


Fig. 4 Re dependency of C_{Lmax} , C_{Dmax} and α_{max} in Reference [2]: (a) C_{Lmax} , C_{Dmax} vs Re , (b) α_{max} vs Re

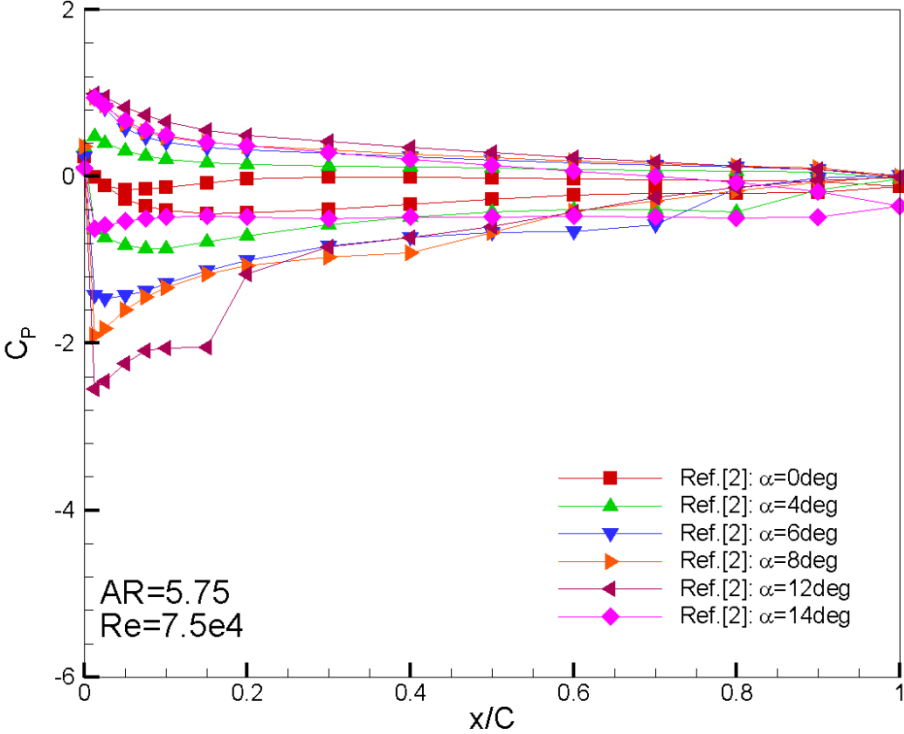


Fig. 5 Trend of C_p in Reference [2]

2.3 Reference [3]

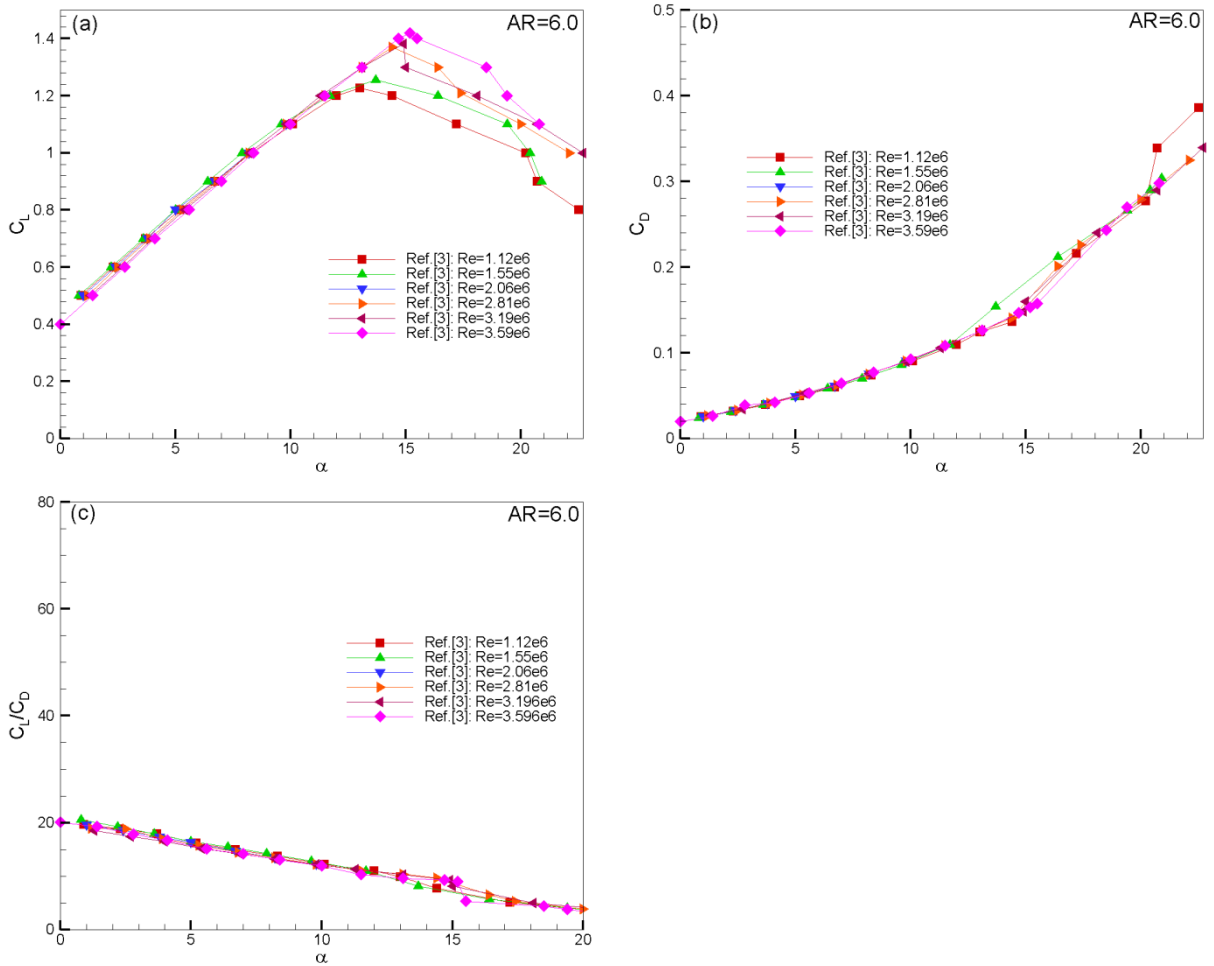


Fig. 6 Trend of C_L , C_D , and C_L/C_D with variations of Re in Reference [3]
 (a) C_L vs α , (b) C_D vs α , (c) C_L/C_D vs α

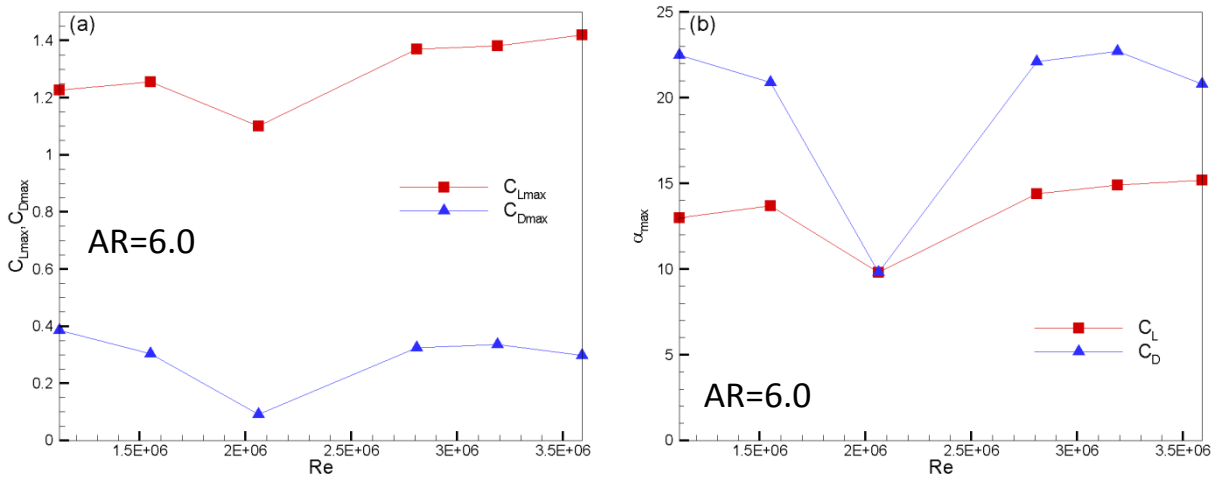


Fig. 7 Re dependency of C_{Lmax} and α_{max} for C_L in Reference [3]: (a) C_{Lmax} vs Re , (b) α_{max} vs Re

2.4 Reference [4]

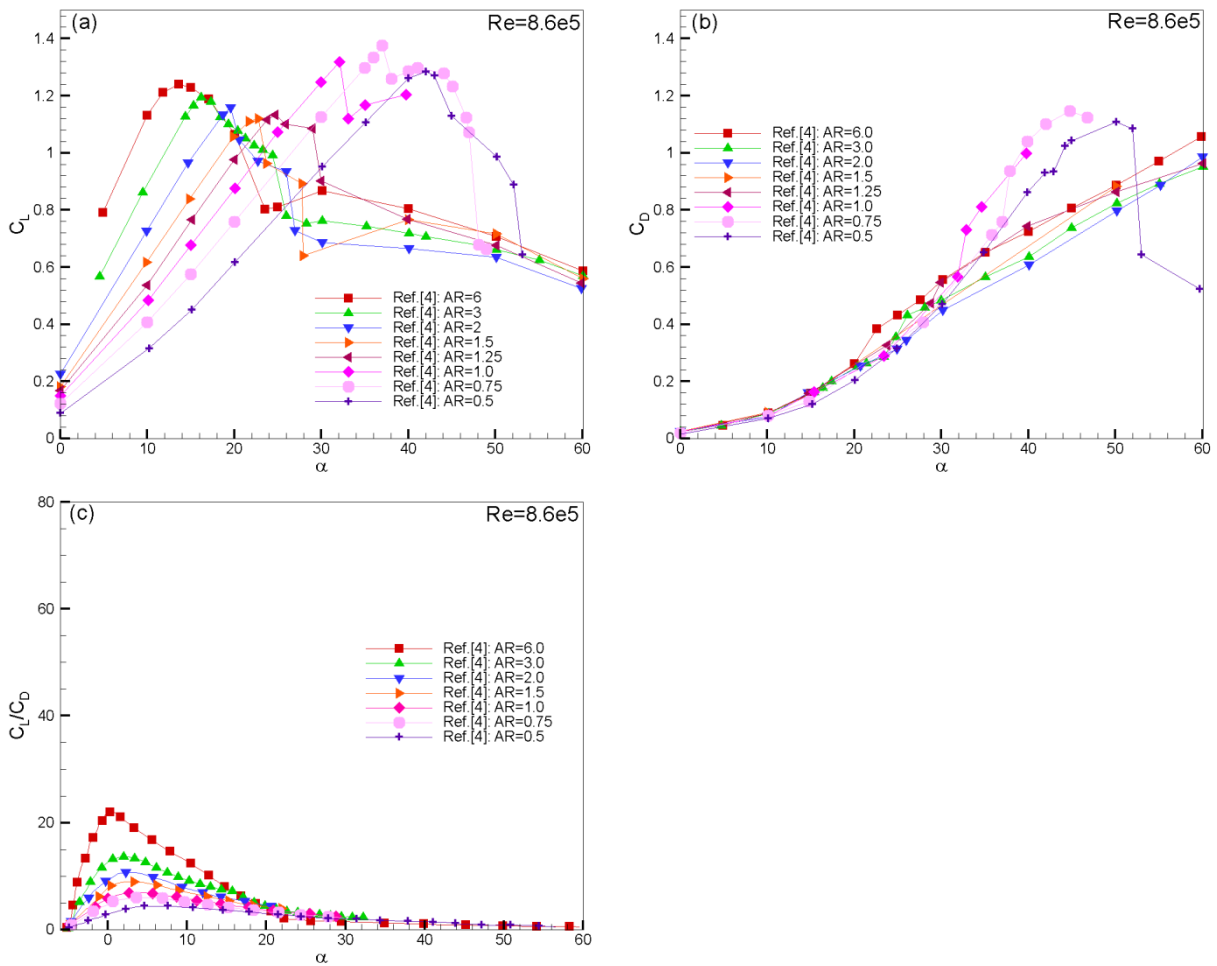


Fig. 8 Trend of C_L , C_D , and C_L/C_D with variations of AR in Reference [4]
 (a) C_L vs α , (b) C_D vs α , (c) C_L/C_D vs α

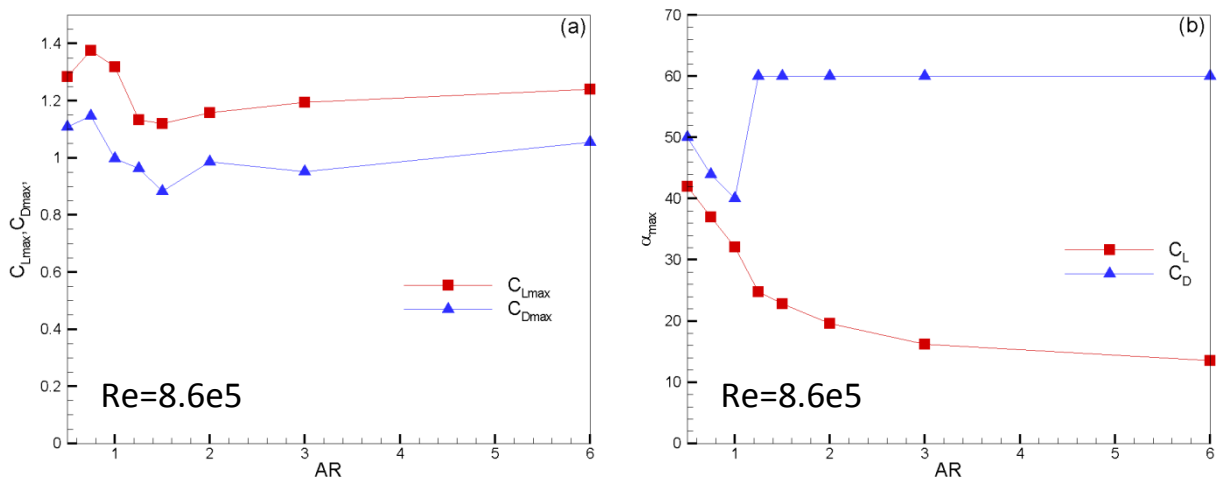


Fig. 9 Aspect ratio dependency of C_{Lmax} and α_{max} for C_L in Reference [4]: (a) C_{Lmax} vs AR, (b) α_{max} vs AR

3. Comparison between the reference experimental data

3.1 C_L vs α with largest AR

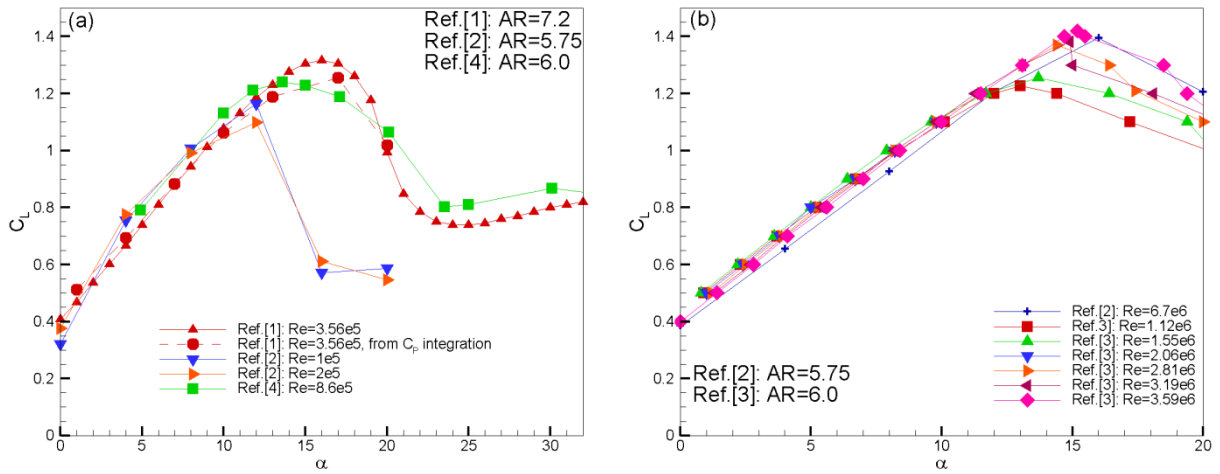


Fig. 10 C_L vs α with largest AR: (a) $Re=O(10^5)$, (b) $Re=O(10^6)$

3.2 C_D vs α with largest AR

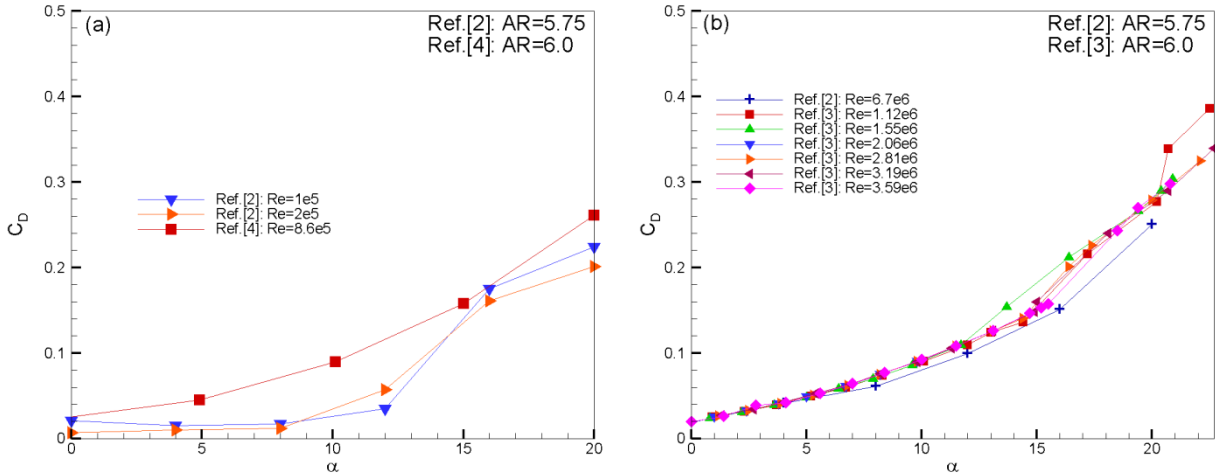


Fig. 11 C_D vs α with largest AR: (a) $Re=O(10^5)$, (b) $Re=O(10^6)$

3.3 C_L/C_D vs α with largest AR

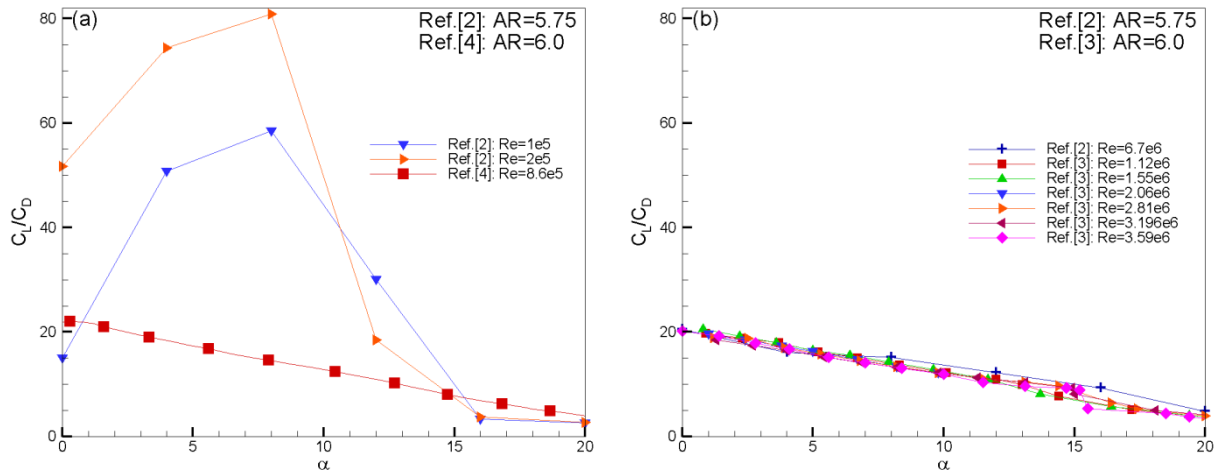


Fig. 12 C_D vs α with largest AR: (a) $Re=O(10^5)$, (b) $Re=O(10^6)$

3.5 C_{Lmax} , C_{Dmax} and α_{max} with largest AR

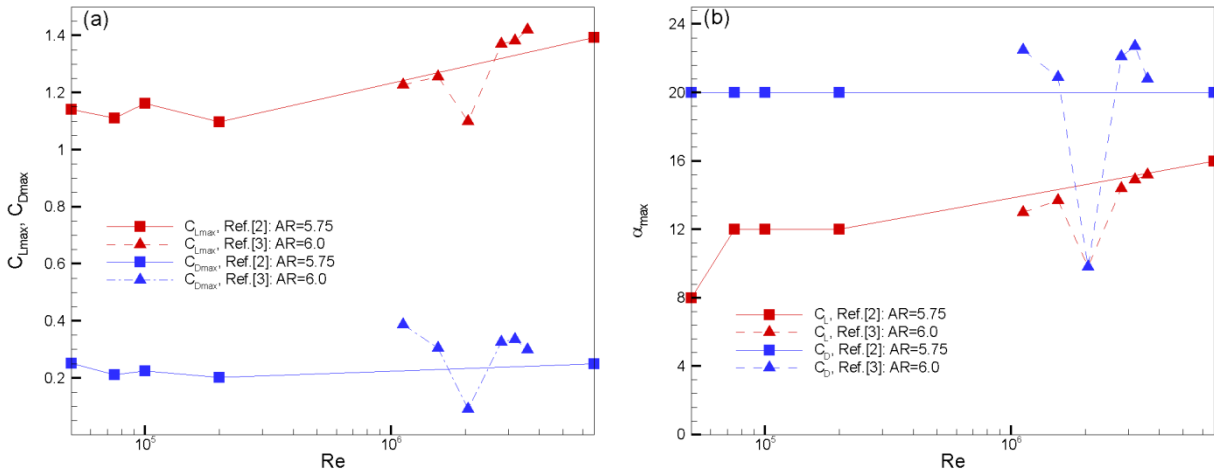


Fig. 13 Re dependency for C_{Lmax} , C_{Dmax} and α_{max} : (a) C_{Lmax} , C_{Dmax} vs Re, (b) α_{max} vs Re

3.4 C_p with largest AR

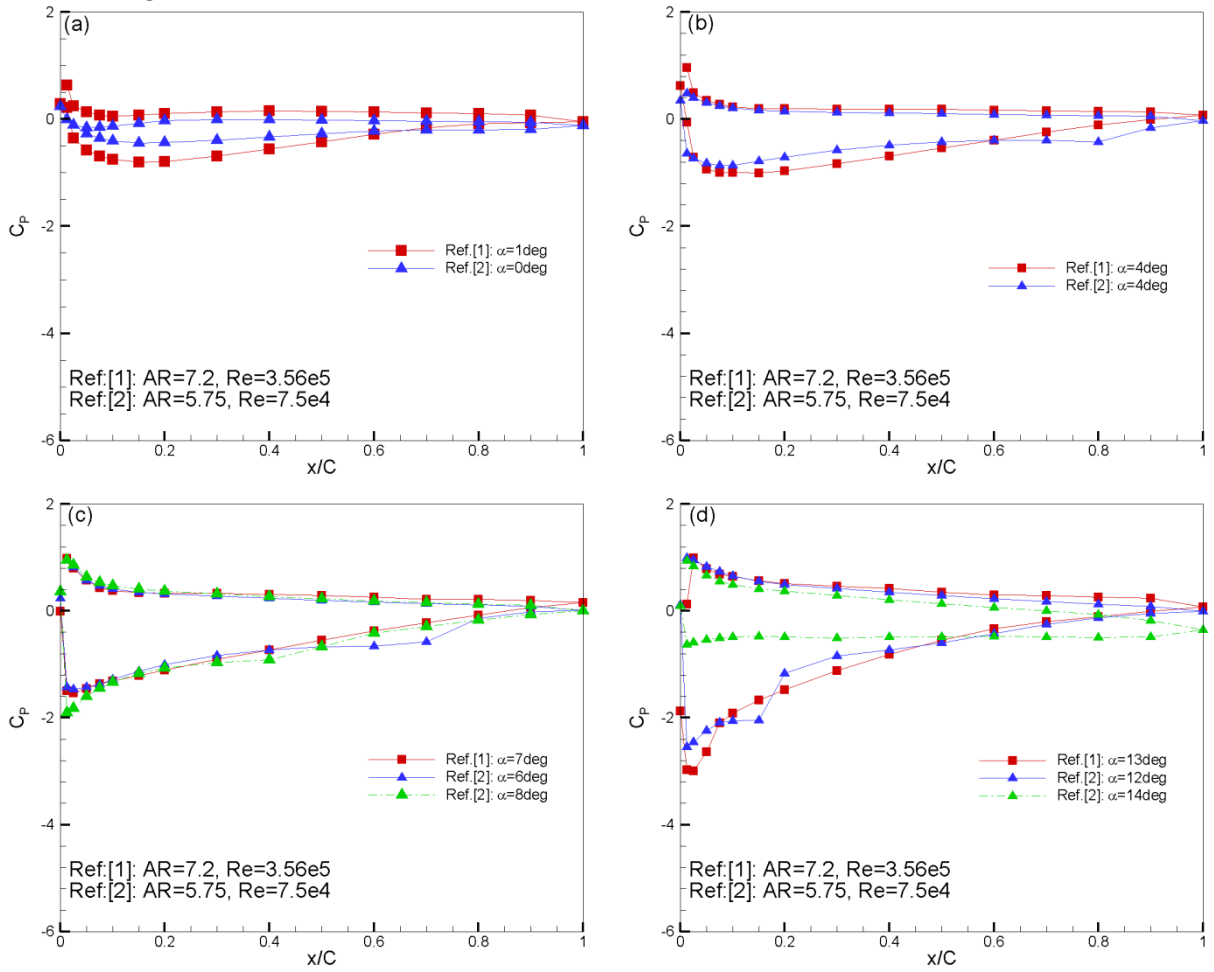


Fig. 14 C_p distribution with largest AR: (a) $\alpha \approx 0^\circ$, (b) $\alpha \approx 4^\circ$, (c) $\alpha \approx 7^\circ$, (d) $\alpha \approx 13^\circ$

4. Comparison with Flowlab simulation results

4.1 C_L vs α

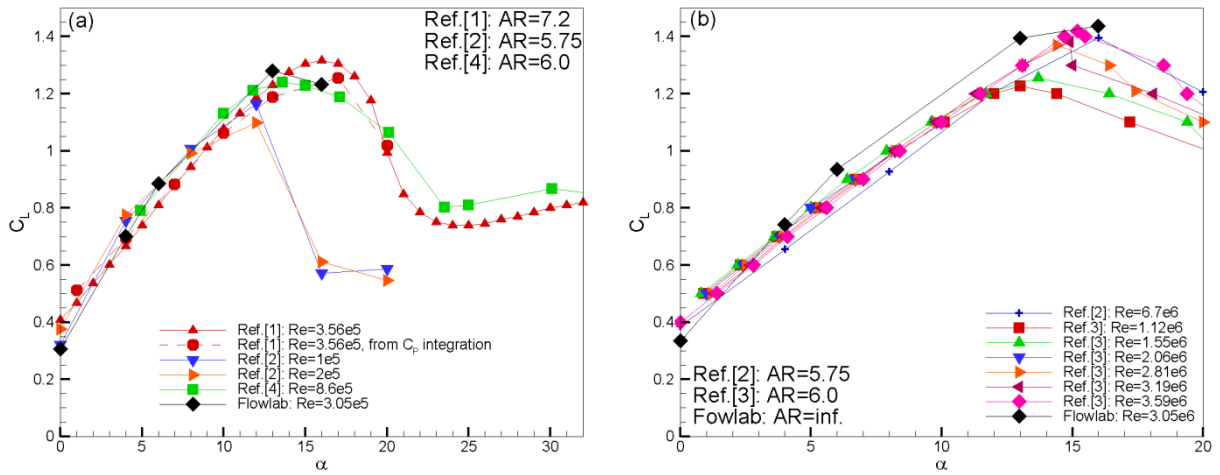


Fig. 15 C_L vs α with largest AR, Flowlab solutions added: (a) $Re = O(10^5)$, (b) $Re = O(10^6)$

4.2 C_D vs α

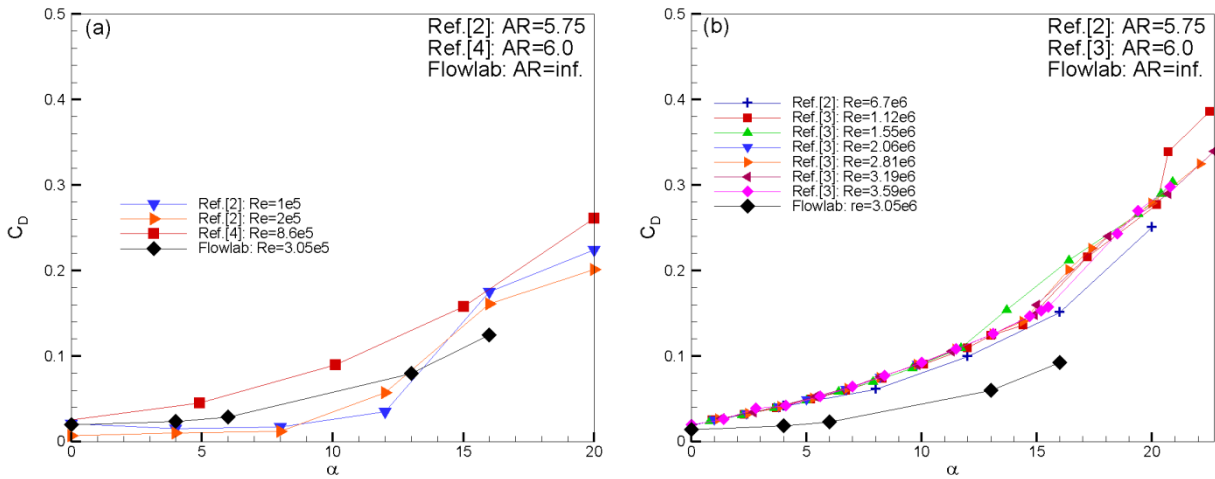


Fig. 16 C_D vs α with largest AR, Flowlab solutions added: (a) $Re = O(10^5)$, (b) $Re = O(10^6)$

4.3 C_L/C_D vs α

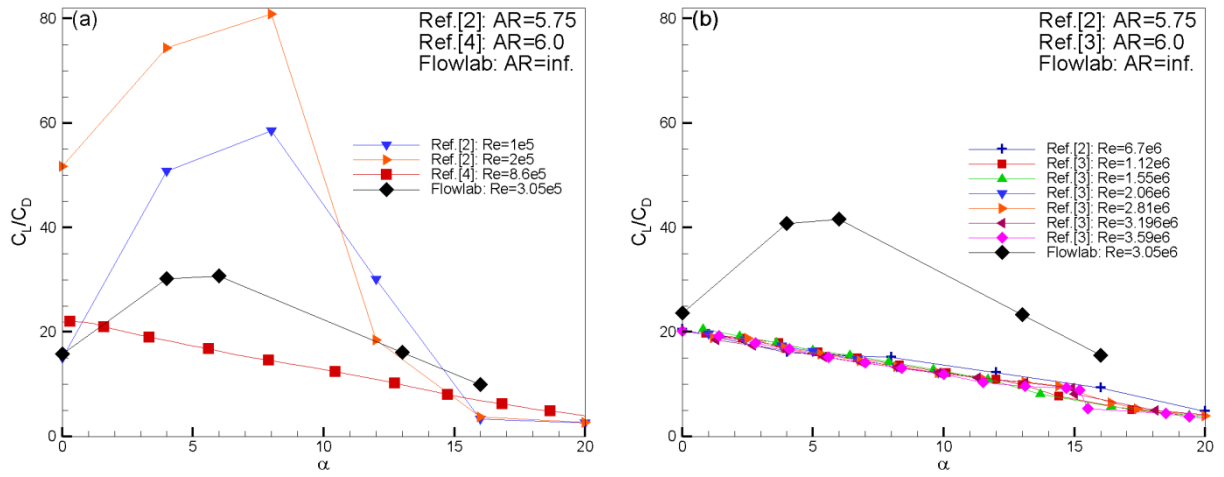


Fig. 17 C_D vs α with largest AR, Flowlab solutions added: (a) $Re=O(10^5)$, (b) $Re=O(10^6)$

4.3 C_p with largest AR

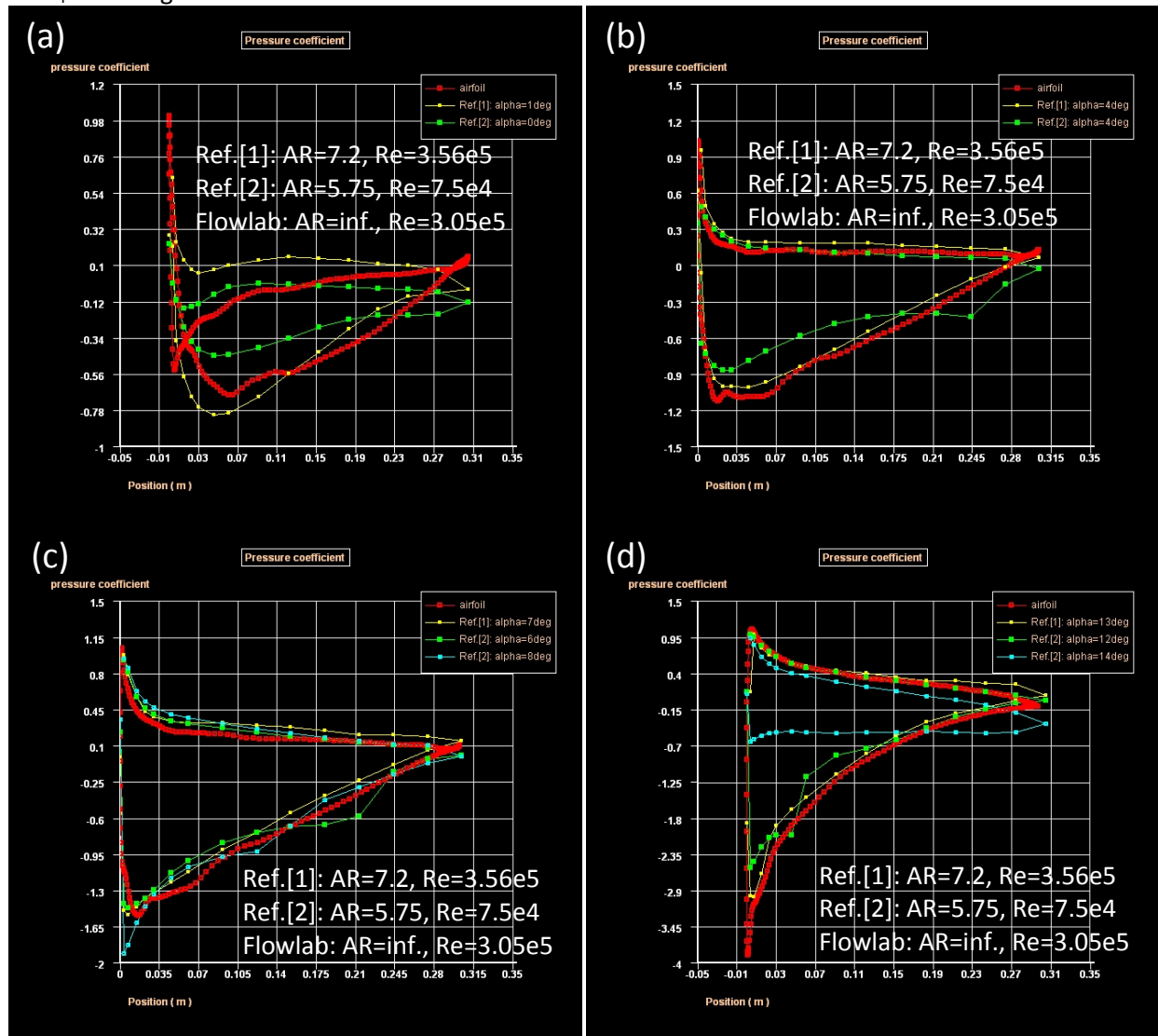


Fig. 18 C_p distribution with largest AR, Flowlab solutions added
 (a) $\alpha \approx 0^\circ$, (b) $\alpha \approx 4^\circ$, (c) $\alpha \approx 7^\circ$, (d) $\alpha \approx 13^\circ$

5. Comparison between EFD benchmark data and IIHR experimental data

5.1 C_L vs α

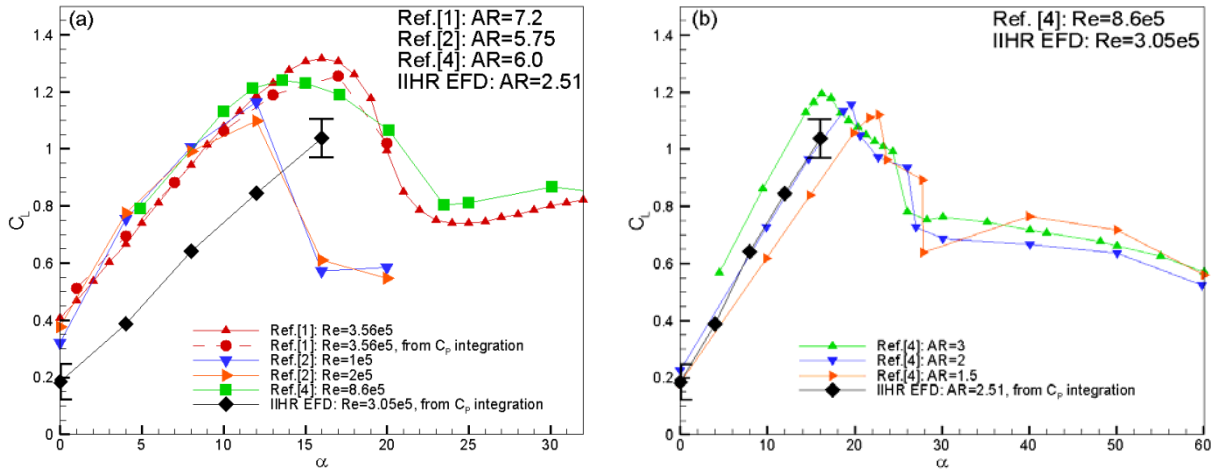


Fig. 19 C_L vs α , IIHR EFD data added: (a) large AR (≥ 5.75), (b) small AR ($1.5 \leq AR \leq 3$)

5.2 C_D vs α

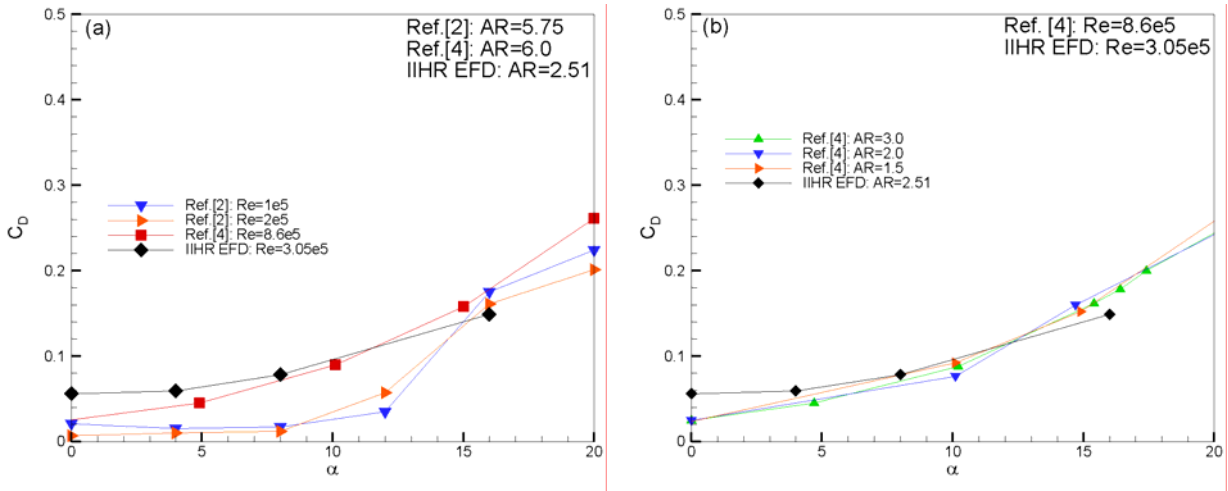


Fig. 20 C_D vs α , IIHR EFD data added: (a) large AR (≥ 5.75), (b) small AR ($1.5 \leq AR \leq 3$)

5.3 C_p

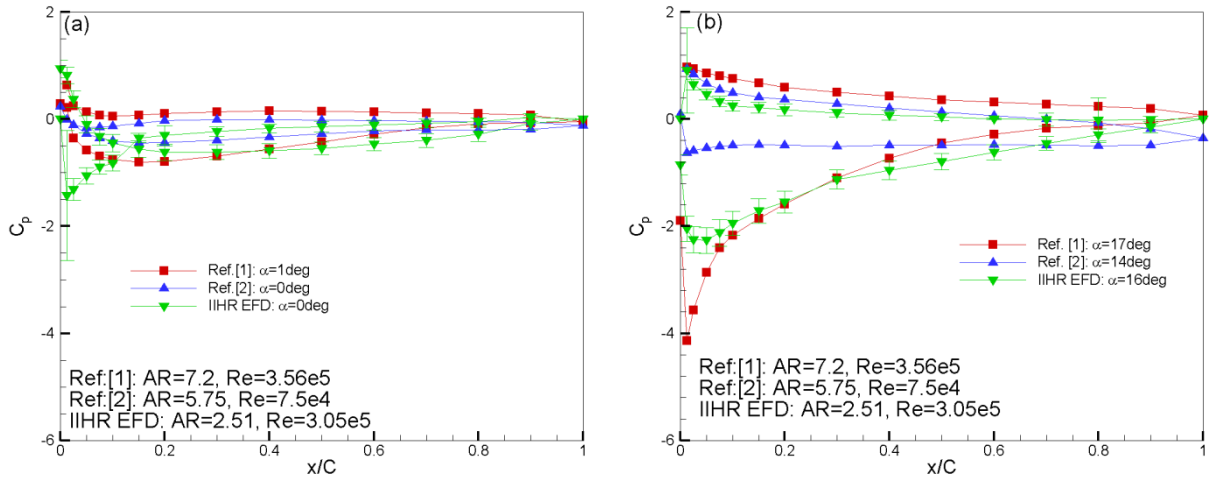


Fig. 21 C_p distribution, IIHR EFD data added: (a) $\alpha \approx 0\text{deg}$, (b) $\alpha \approx 16\text{deg}$

6. Comparison between EFD benchmark data, IIHR experimental data and Flowlab solution

6.1 C_L and C_D vs α

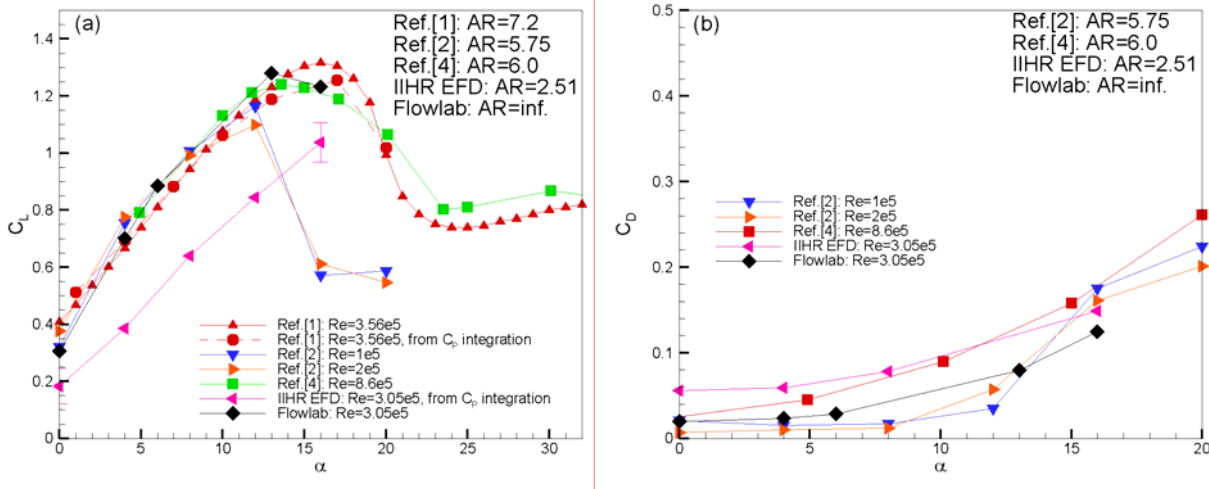


Fig. 22 C_L and C_D vs α : (a) C_L , (b) C_D

6.2 C_p

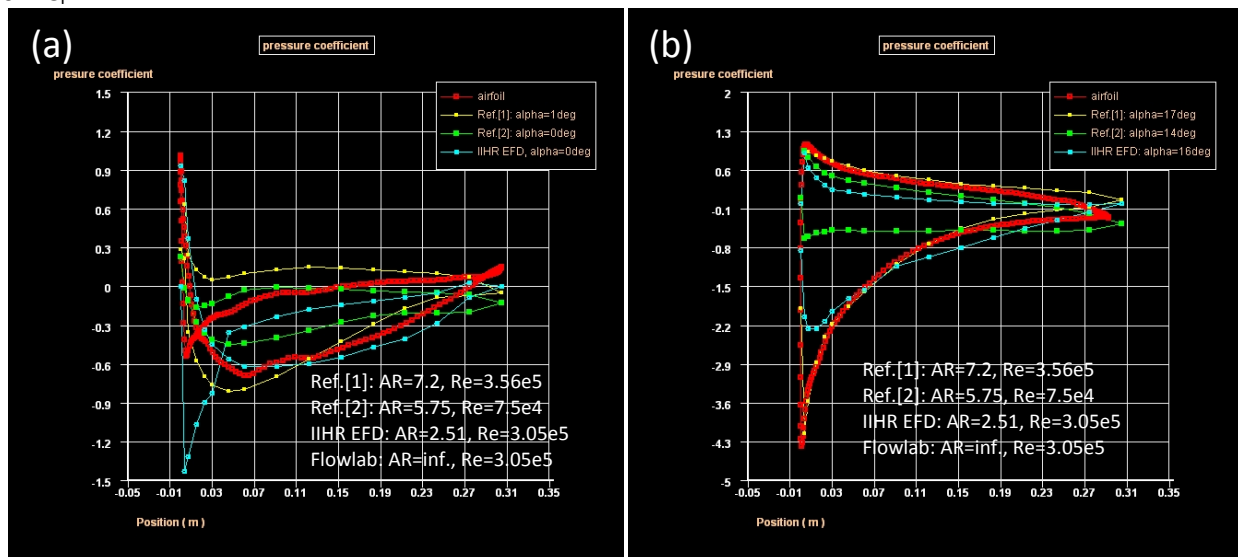


Fig. 23 C_p distribution: (a) $\alpha \approx 0$ deg, (b) $\alpha \approx 16$ deg

7. Discussion and Conclusion (To be added.)